The Journal of Neuroscience, October 1993, 13(10): 4403–4411

# Extracellular ATP Activates a Cation Conductance and a $K^+$ Conductance in Cultured Microglial Cells from Mouse Brain

**W. Walz,[1] S. Ilschner,[2] C. Ohlemeyer,[2] R. Banati,[3] and H. Kettenmann[2]**

[1]Department of Physiology, University of Saskatchewan, Saskatoon, Saskatoon S7N 0W0, Canada, [2]Institut für Neurobiologie der Universität, W-6900 Heidelberg 1, Germany, and [3]Max-Planck-Institut für Psychiatrie, W-8033 Planegg-Martinsried, Germany

**Microglial cells have important functions during regenerative processes after brain injury. It is well established that they rapidly respond to damage to the brain tissue. Stages of activation are associated with changes of cellular properties such as proliferation rate or expression of surface antigens. Yet, nothing is known about signal substances leading to the rapid changes of membrane properties, which may be required to initiate the transition from one cell stage into another. From our present study, using the patch-clamp technique, we report that cultured microglial cells obtained from mouse or rat brain respond to extracellularly applied ATP with the activation of a cation conductance. Additionally, in the majority of cells an outwardly directed $K^+$ conductance was activated with some delay. Since ADP, AMP, and adenosine (in descending order) were less potent or ineffective in inducing the cation conductance, the involvement of a $P_2$ purinergic receptor is proposed. The receptor activation is accompanied by an increase of cytosolic $Ca^{2+}$ as determined by a fura-2–based $Ca^{2+}$-imaging system. This ATP receptor could enable microglial cells to respond to transmitter release from nerve endings with ATP as a transmitter or cotransmitter or to the death of cells with resulting leakage of ATP.**

***[Key words: microglia, ATP, purinergic receptor, fura-2 imaging, patch clamp, ion channels]***

Microglia (or brain macrophages) are known to have important functions during immunological processes, ontogenesis, and regeneration in the CNS (Giulian and Ingeman, 1988; Perry and Gordon, 1988; Streit et al., 1988; Banati et al., 1991; Gehrmann et al., 1992). Under normal conditions in the adult brain, they appear as resting microglia characterized by an elaborate morphology and an antigenic profile distinct from activated forms of microglia. Activated microglia can be observed after damage to the nervous system, during infections or development, or in culture (Ramon y Cajal, 1914; Giulian and Baker, 1986; Leist et al., 1988; Graeber et al., 1989). Activation can result in a spectrum of morphological and functional changes, including proliferation or phagocytosis, which can occur in sequential stages in a model of CNS injury (Kreutzberg, 1978). Additional properties of microglial cells can be used to characterize their state of activation, for example, presence of major histocompatibility complex class II (MHC II) antigen (Streit et al., 1989), acetylated low-density-lipoprotein (ac-LDL) receptors (Giulian and Ingemann, 1988), or tumor necrosis factor production (Frei et al., 1978). Nothing is yet known about the signals from damaged neurons that would induce the transition from one state of cell activation into another.

To assess properties of microglia, cell culture systems have been developed that yield purified populations of microglial cells (Frei et al., 1978; Giulian and Baker, 1986). Using the patch-clamp technique, membrane channels of cultured rat microglial cells were studied. In this cell population ion channels were expressed in a pattern that is distinct from neurons and macroglial cells on the one hand, and from peripheral macrophages on the other (Kettenmann et al., 1990). An inwardly rectifying current and practically no outward currents were observed. Small inward currents can lead to a large membrane depolarization since $K^+$ outward currents are not activated with depolarization. Membrane potential changes have been found to be associated with cell attachment and phagocytosis in monocytic cells (Gallin and Gallin, 1977; Gallin and Sheehy, 1985), but no substance is known that would elicit electrical membrane responses in microglia. Also, the intracellular calcium concentration has been monitored in macrophages and leukocytes during processes like phagocytosis or proliferation whereby transient increases or oscillations in the $Ca^{2+}$ concentration preceded morphological changes (Kruskal et al., 1986; Kruskal and Maxfield, 1987; Metcalfe et al., 1990; Rephaeli et al., 1990; di Virgilio et al., 1991; Meagher et al., 1991). A putative signal substance could influence a microglial cell by changing its membrane potential as well as the intracellular calcium concentration.

In this study we investigated the effects of ATP on microglial cells. This compound is released in the CNS as a cotransmitter from neurons and as a modulatory substance from endothelial cells (Burnstock, 1990). Furthermore, ischemic, injured, and dying cells release ATP in large amounts (Imai et al., 1964; Forrester and Williams, 1977). In peritoneal macrophages and in lymphocytes, extracellular ATP has the potential to play a role in cell activation, since it has been shown to stimulate transmembrane ion fluxes and intracellular calcium changes in these cells (Cameron, 1984; Steinberg and Silverstein, 1987). Thus, extracellular ATP has to be regarded as a prime candidate for a signal substance to trigger functional changes in microglia.

## Materials and Methods

*Cell culture—microglia.* Cultures of microglial cells were prepared from embryonic day 16 (E16) mouse brain or newborn rat brain essentially as described previously (Frei et al., 1978; Giulian and Baker, 1986).

Received Nov. 2, 1992; revised Feb. 17, 1993; accepted Apr. 15, 1993.

Correspondence should be addressed to Helmut Kettenmann, Institut für Neurobiologie, Universität Heidelberg, Im Neuenheimer Feld 345, W-6900 Heidelberg 1, Germany.

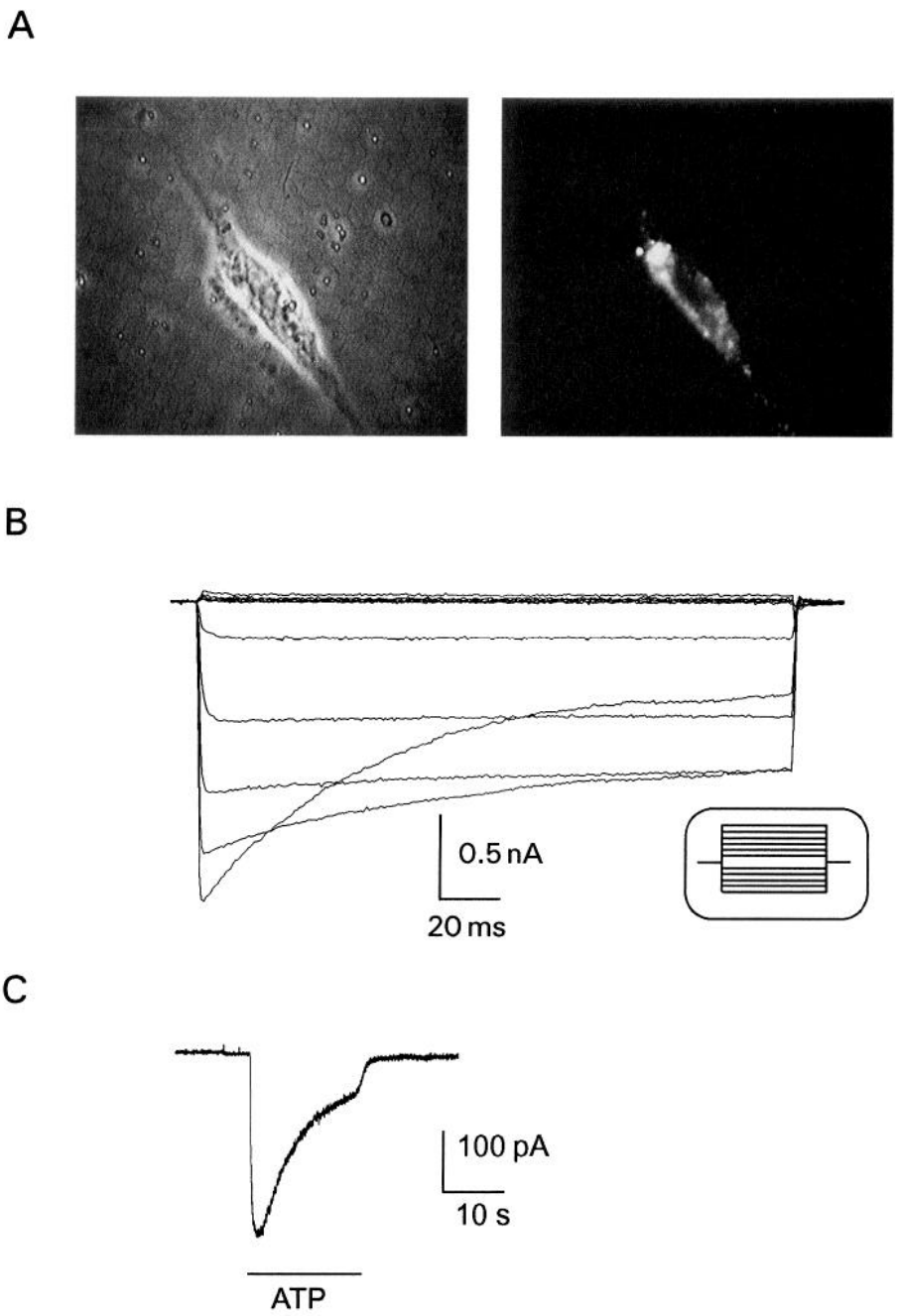


*Figure 1.* Identification of microglial cells and ATP-induced membrane current. *A,* A microglial cell replated from cultures of the mouse cortex is shown in phase contrast (*left*) and stained with DiI–ac-LDL (*right*). The pictures were obtained with an imaging system that was used for the $Ca^{2+}$ measurements as shown in Figures 5–7. *B,* Membrane currents were recorded from a microglial cell. The membrane potential was clamped at −70 mV and jumped for 200 msec to de- and hyperpolarizing values ranging from 50 to −170 mV with 20 mV increments as displayed in the *inset* on the *lower right*. This current pattern is typical for cultured microglial cells (Kettenmann et al., 1990). *C,* Effect of 100 μM ATP on membrane currents. The membrane was clamped at −70 mV and ATP was applied for 20 sec as indicated by the *bar*.

Following mechanical dissociation of the tissue in Dulbecco's modified Eagle's medium (DMEM) supplemented with 2 gm/liter $NaHCO_3$ and 20% heat-inactivated fetal calf serum, primary cultures were kept in 75 $cm^2$ culture flasks at 3% or 5% $pCO_2$ and 37°C for 2–4 weeks. In the mouse brain cultures, neurons were killed with a complement reaction after 5 d in culture (Trotter et al., 1989). Cells growing on top of a confluent cell layer were removed by rotary shaking and plated on glass coverslips with a mean plating density of $2 \times 10^5$ cells/$cm^2$ for mouse and of $2 \times 10^4$ cells/$cm^2$ for rat. Plated cells were kept in the same medium for 1–7 d before recording.

*Cytochemical methods.* For identification of mouse microglia cells, a method using DiI–acetylated low density lipoproteins (DiI–ac-LDL) (Giulian and Baker, 1986) from Paesel and Lorei (Frankfurt, Germany) was applied. Previous to several electrophysiological or calcium-imaging experiments, cells were incubated in their culture medium with 10 μg/ml DiI–ac-LDL for 4 hr and viewed with the rhodamine filter set of the $Ca^{2+}$-imaging setup (see below). For validation of this labeling, immunocytochemistry with anti-CD45 and Mac-1 antibody (both from Boehringer Mannheim), diluted 1:200 and 1:100 in PBS, respectively, was performed on previously DiI-ac-LDL–labeled cells after 2% paraformaldehyde fixation (5 min). To exclude the possibility of astrocytes having taken up DiI–ac-LDL as well as microglia, a second double staining was done, combining DiI–ac-LDL with polyclonal anti–glial fibrillary acid protein antibody (anti-GFAP) (Dako Diagnostika, Hamburg, Germany), diluted 1:200. Cells were permeabilized with *n*-octylglucopyranoside (Boehringer Mannheim) before application of GFAP antibody.

Also, rat microglial cells were prepared and identified as described (Kettenmann et al., 1990). Cells submitted to immunocytochemistry after fixation in phosphate-buffered formaldehyde (3.7%, 5 min) and in acetone (50%, 2 min; 100%, 3 min; 50%, 2 min). The MRC OX-41, OX-42 monoclonal antibodies were obtained from Serotec (Camon), Wiesbaden, Germany. The monoclonal antibody against GFAP was purchased from Boehringer Mannheim. The working dilution in 0.01 M Tris-buffered saline (TBS) was 1:50 for all antibodies. Visualization was carried out using the Vector ABC–alkaline phosphatase standard

kit. Fast red TR salt (1 mg/ml; Sigma, F-1500) dissolved in naphthol-AS-MX phosphate (0.2 mg/ml; Sigma, N-5000)/Tris-HCl buffer (0.1 M, pH 8.2) containing 1 mM levamisole (Sigma, L-9756) was used as a substrate solution.

*Recording setup and solutions.* Cultures were maintained on the stage of an inverted microscope at about 25°C. The cultures were superfused with a standard salt solution containing (in mM) KCl, 5.4; NaCl, 150; $MgCl_2$, 1; $CaCl_2$, 2; glucose, 10; and HEPES, 5. The pH was adjusted to 7.3. To alter $[K^+]_o$, NaCl was replaced by KCl. Low-chloride solution was made by substitution of NaCl and KCl with Na- and K-gluconate, and low-sodium solution, by using choline chloride. ATP, ADP, AMP, and adenosine were obtained from Sigma, kept as frozen 100 mM stock solutions, and diluted as described before each experiment.

*Patch-clamp procedures.* Whole-cell currents were recorded applying the patch-clamp technique (Hamill et al., 1981). Currents were amplified with an EPC-7 amplifier (List, Darmstadt, Germany). Recording pipettes contained (in mM) KCl, 130; $MgCl_2$, 1; $CaCl_2$, 1; EGTA, 10; and HEPES, 10. The pH was adjusted with KOH to 7.4. The resistance of the pipettes varied from 4 to 10 MΩ. The holding potential was −70 mV. Data were taken with sampling rates from 100 Hz up to 5 kHz and filtered at 3 kHz.

*Data processing.* Data were digitized by an interface card connected to an AT-compatible computer. A Pascal program developed in our laboratory was used to analyze and display the recorded traces. The computer was also connected to the voltage-clamp control of the patch-clamp amplifier and could perform sequences of voltage steps and voltage ramps during recording.

*Calcium imaging.* Cells on coverslips were incubated at room temperature for 25 min with fura-acetoxymethyl ester, or for 5 min at 4°C and then at room temperature for 20 min. On the stage of a Zeiss axioplan microscope fura-2–loaded cells were perfused with either calcium-free or calcium-containing bath solution. For application of substances a system of plastic tubing running as parallel pathways to the bath perfusion was used. Fura-2 was excited at 340 and 380 nm. Fluorescence, filtered through a bandpass filter transmitting 500–530 nm, was detected by an intensified CCD camera (Hamamatsu). Ratio images were calculated in real time and stored on hard disk for further processing. For perforated-patch recordings, nystatin was used in the pipette according to the method of Korn et al. (1991) in one set of experiments.

## Results

### *Cytochemical and physiological identification of cells*

We used two strategies to identify microglial cells in culture, namely, by cell-type-specific staining methods and by recording the voltage-activated currents. The cells in this culture system were positively stained with DiI–ac-LDL (Fig. 1*A*) and with the antibodies Mac-1 or CD-45 as markers for microglial cells in the brain. Only occasionally unstained cells were seen, most likely oligodendrocytes, glial precursor cells, or astrocytes (less than 1%). As demonstrated with double stainings using anti-GFAP antibody for identification of astrocytes, and DiI–ac-LDL, no astrocytes stained with DiI–ac-LDL. In contrast to the large variabilities in shape, membrane currents were similar in the vast majority of microglial cells from that culture system: while depolarizing voltage steps did not activate any currents (holding potential at −70 mV), hyperpolarizing steps elicited large inward currents as previously described (Kettenmann et al., 1990; Fig. 1*B*).

### *Properties of the ATP-activated current*

Membrane currents were recorded using the patch-clamp technique in the whole-cell configuration while clamping the membrane at −70 mV. Application of 100 μM ATP elicited an inward current with a mean peak amplitude of 98 pA (Fig. 1; $n = 57$; range, 7–972 nA). Part of the ATP inward current desensitized during the ATP application. The degree of desensitization varied; after an application for 20 sec the washout of ATP caused a termination of the induced inward current. In most cells the residual current was less than 20% of the peak current after a 60 sec application.

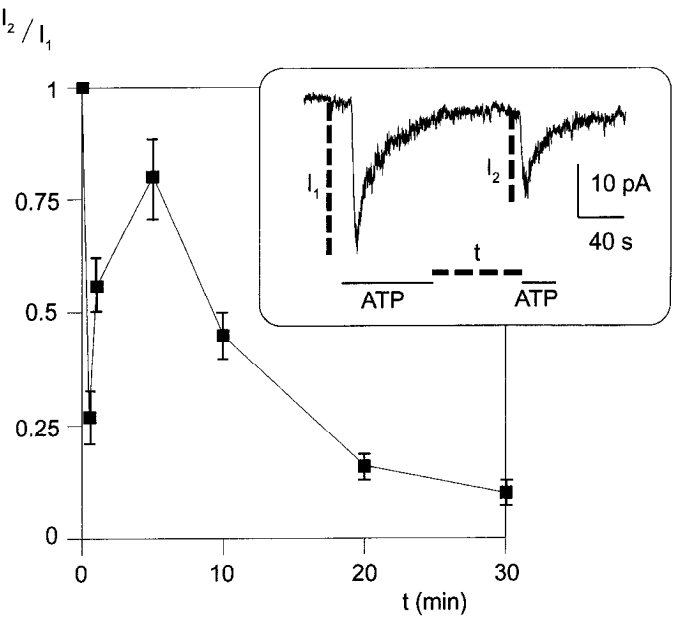


*Figure 2.* Recovery of the ATP response. The graph displays the relationship of the time between two subsequent ATP applications ($t$) and the relative amplitude ($I_2/I_1$), with standard error, of the pairs of responses. The delay time was 0.5, 1, 5, 10, 20, or 30 min. The *inset* shows an example of a recording with a delay of 60 sec.

### *Time course of current amplitudes after repeated application of ATP*

After a first application of ATP, a second ATP application was given at six different time points 0.5–30 min later (Fig. 2). The relationship of the second to the first amplitude changed in a biphasic way. There is a long-lasting "rundown" of the response with a half-time of about 8 min. Superimposed on this time course is a much faster desensitization that is maximal in the first minute after the first application and that is no longer present after 5 min.

### *Conductance change and reversal potential of the ATP response*

We measured the ATP-induced currents at different membrane potentials to determine the reversal potential and the conductance of the ATP response (Fig. 3*A*). From the holding potential of −70 mV, the membrane was clamped at −105, −35, 0, and 35 mV for 100 msec with a time interval between the jumps of 100 msec. This protocol was repetitively applied every 3.6 sec. From the corresponding current values, current–voltage relationships were constructed, allowing the repetitive monitoring of the membrane conductance changes prior to and during application of ATP (100 μM). ATP evoked a biphasic conductance change: within the first 5 sec after the onset of the ATP response the conductance increase in the hyperpolarizing direction reached its peak; the conductance increased by 2.17 nS (mean value; $n = 26$; range, 0.5–14.6 nS). The current–voltage curve of the ATP-induced current was linear and the reversal potential of the current response was 0 mV (mean value; $n = 24$; range, −35 to +8 mV; see Fig. 3). Subsequently, the ATP-induced current decreased at −70 and −105 mV, but increased at more positive potentials. The peak of the current increase in the depolarizing

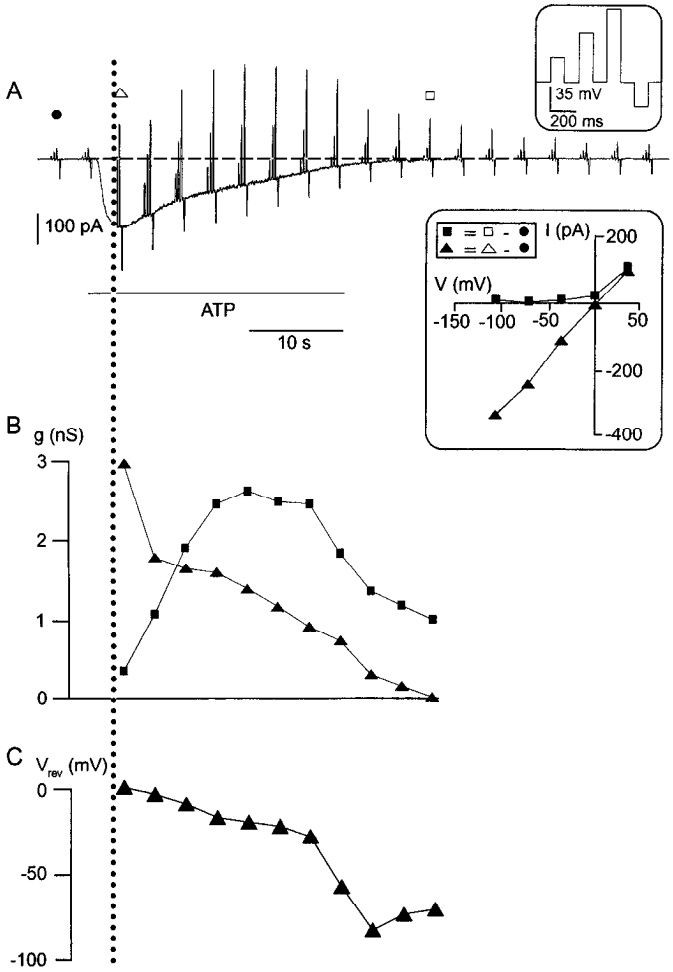


*Figure 3.* ATP-induced conductance and reversal potential. *A*, Membrane currents were recorded at different potentials while ATP (100 μM) was applied as indicated by the *bar*. With a voltage-clamp protocol, the membrane was repetitively depolarized or hyperpolarized for 100 msec intervals to −35, 0, +35, and −105 mV from a holding potential of −70 mV. A single sequence of voltage steps is illustrated in the *upper inset* in an expanded time frame. This clamp protocol was repetitively applied. The *lower inset* illustrates current–voltage curves, constructed from the recording shown in *A*. Currents at two indicated time points during the ATP response were substracted from currents recorded prior to the ATP application. We thus display the ATP-activated currents: the one at the peak of the inward current is shown by the *triangles*, while the ATP induced outward current at the late phase of the ATP response is illustrated by *squares*. *B*. Current responses to the voltage step from −70 to −105 mV were measured from the recording shown in *A*, during a number of sequences of voltage steps. The current response in the control solution was subtracted from those in presence of ATP and conductances (*g*) were calculated. We thus obtained the conductance increase in hyperpolarizing direction (*triangles*), which reflects the conductance increase induced by the cation channel. To assess the additional conductance increase induced by the activation of the $K^+$ conductance, the conductance increase in hyperpolarizing direction was subtracted from the conductance increase in depolarizing direction (*squares*). *C*, From the current–voltage curves as shown in the *inset* in *A*, the ATP current reversal potential ($V_{rev}$) was determined during the course of the ATP response. The reversal potential slowly shifts from 0 mV to −70 mV, indicating the transition from the cation-selective to the $K^+$-selective conductance.

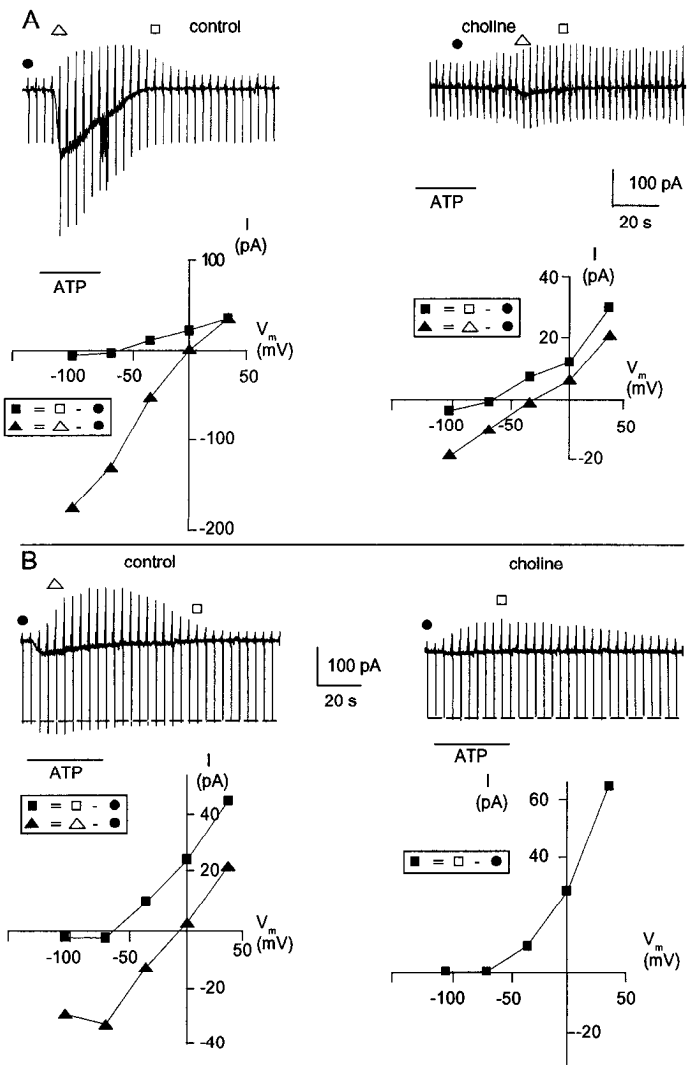


*Figure 4.* Ionic dependence of the ATP-induced current—effect of $Na^+$ substitution by choline. *A*, With a voltage-clamp protocol as described for Figure 3, membrane currents were measured at different membrane potentials while ATP (100 μM) was applied. The *left trace* shows the response in control solution; the *right trace*, in low-$Na^+$/high-choline–containing solution. Current (*I*)–voltage (*V*) curves were constructed by subtracting the voltage jumps in normal solution from the recordings shown at the peak of the ATP-induced inward current (marked by a *triangle*) and at the late phase of the ATP response (*square*). The *graph at the left* was obtained from the control response; the *graph at the right*, in low-$Na^+$-high-choline–containing solution. The reversal potential of the fast current response shifted from 0 to −38 mV, while the reversal potential of the slow current response stays at about −60 mV. *B*, Similar to *A*, ATP-induced currents were recorded from a different cell that showed a less prominent ATP-induced inward current at the holding potential (−70 mV). In the low-$Na^+$/high-choline–containing solution the inward current can no longer be observed.

direction was reached within the first 10 sec. While the current at −70 mV and −105 mV had returned to the resting level, the current in the depolarizing direction was still increased. The current–voltage curve at this late phase revealed a conductance increase at potentials positive to −40 mV (Fig. 3*B*). The extrapolated reversal potential was at about −50 mV (mean value; $n = 17$; range, −75 to −20 mV; average, −49 mV), thus in the range of the $K^+$ equilibrium potential (Fig. 3). Figure 3*C* illustrates the transition of the reversal potential from about 0 mV to −70 mV. This curve reflects the change in the dominance of the two current components over time. The relative contribution of the two current components varied among cells. In some cells, a prominent delayed phase was observed, while in others such a component was not obvious (e.g., compare Figs. 3–5).

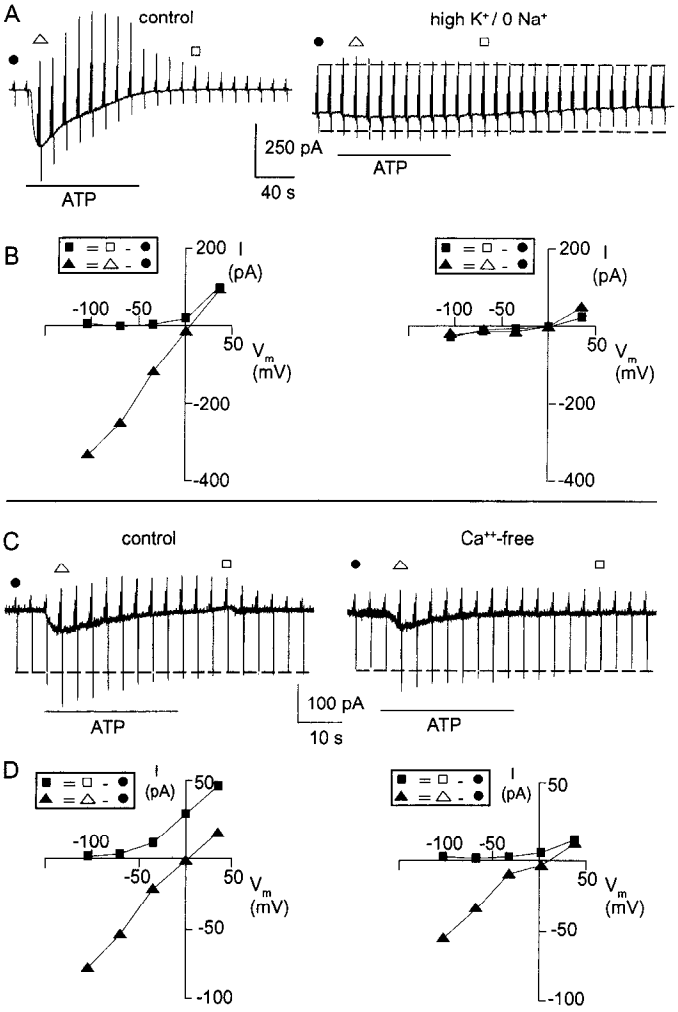


*Figure 5.* Ionic dependence of the ATP-induced current—effect of low $Na^+$ substituted by $K^+$ and effect of low $Ca^{2+}$. *A* and *B*, Membrane currents were recorded and current–voltage curves constructed as described for Figure 3. A control response (*left*) was compared to a response in low $Na^+$/high $K^+$. The ATP-induced current is strongly reduced. The reversal potential of both the fast and the slow current response is at about 0 mV. *C* and *D*, With a similar protocol, the effect of omitting $Ca^{2+}$ (in the presence of 2 mM EGTA; *right traces*) as compared to a control (2 mM $Ca^{2+}$; *left traces*) was analyzed. While the reversal potentials were not affected, the outward currents were reduced in amplitude.

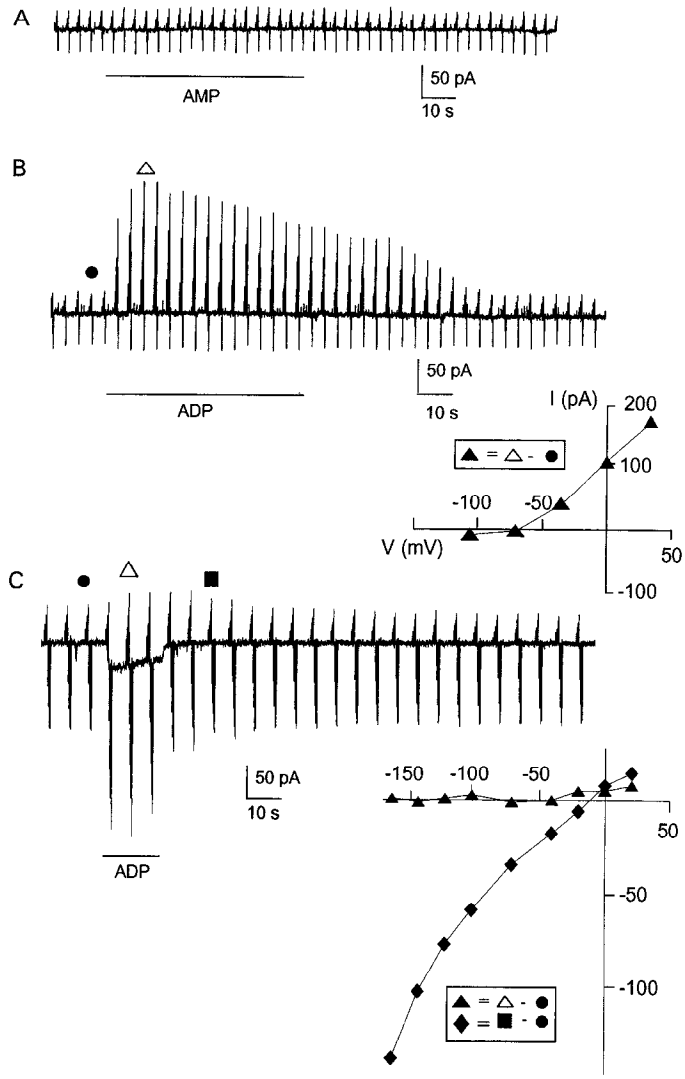


*Figure 6.* Effect of AMP and ADP. *A*, Membrane currents were measured as described for Figure 3. AMP (100 μM) did not induce any current change. *B*, In contrast, application of ADP induced a substantial increase in outward currents in this cell. Depolarizing and hyperpolarizing voltage steps were applied as described for Figure 1. The current–voltage curve of the ADP-induced current was constructed as described for Figure 3 and indicates a reversal potential at about −70 mV. *C*, Another cell responded to ADP with activation of currents resembling the response to ATP as shown in this example. Voltage steps applied to this cell differed from the recordings shown in *B* as can be seen on the current–voltage curve. The two components described for ATP responses can be demonstrated.

### *Ionic dependence of the ATP response*

To reveal the ionic dependence of the ATP-induced current, we compared the reversal potential and conductance change of the ATP response in solutions containing different ion concentrations. We separately evaluated the fast and the slow conductance change to distinguish between these two current components. The reversal potential of the fast current component was obtained at the peak of the inward current. The reversal potential of the slow component was measured at the late phase of the ATP response, when the current responses to hyperpolarizing voltage steps had returned to normal.

To test for the involvement of $Na^+$, extracellular $Na^+$ was substituted by choline; the reversal potential of the fast current component changed from −4.3 to −43.4 mV and the ATP-induced conductance decreased by 88% (mean value; $n$ = 5; Fig. 4). The reversal potential of the second component was not altered ($n$ = 5). Due to the smaller responses, the two current components were not always apparent. Figure 4, *A* and *B*, illustrates recordings from two different cells with a prominent fast and slow component, respectively.

If $Na^+$ was substituted by $K^+$, the reversal potential of the first component was not affected while the reversal potential of the slower component changed to about 0 mV (mean value; $n$ = 5; Fig. 5*A*,*B*). As observed for the substitution of $Na^+$ by choline, the ATP-induced conductance decreased markedly, with a mean of 56%. Substitution of extracellular $Cl^-$ by gluconate did not change the reversal potential for the two current components (not shown; $n$ = 5). Similarly, omitting extracellular $Ca^{2+}$ from the salt solution did not significantly affect the re-

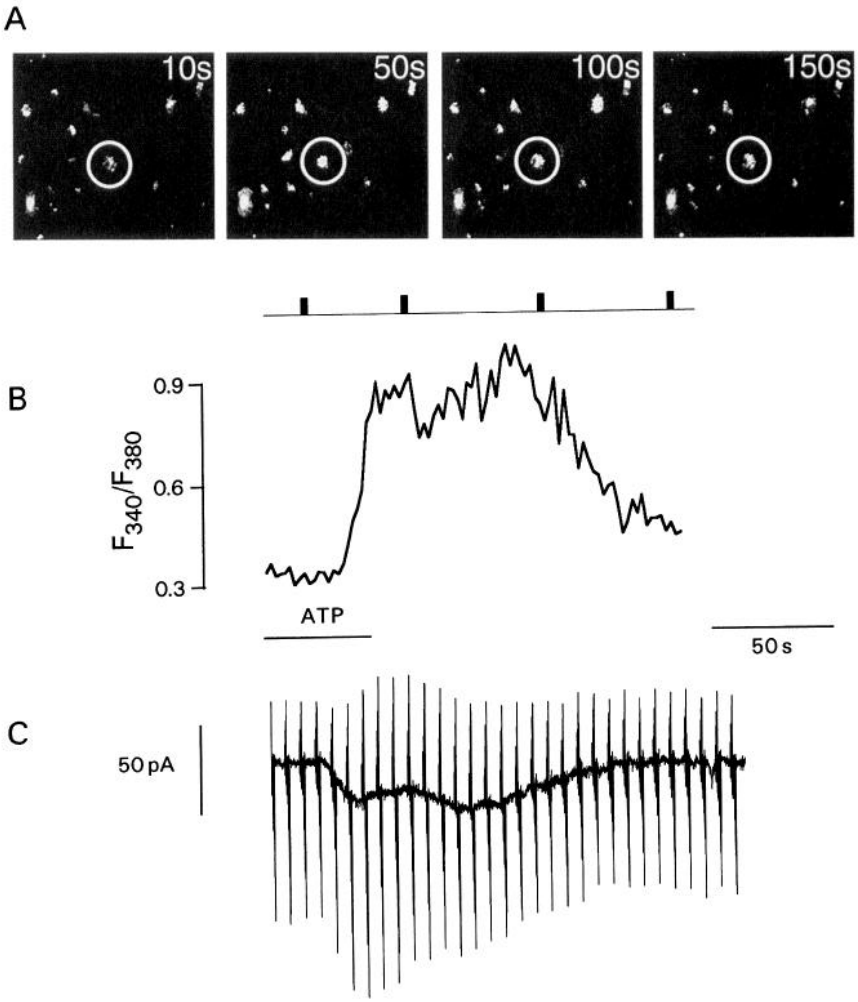


*Figure 7.* $Ca^{2+}$ response to ATP compared with current response. *A*, Images of changes in $[Ca^{2+}]_i$ were obtained using the fura-2 system. Data were sampled at 0.5 Hz and displayed as gray levels. *Lighter shades* indicate an increase in $[Ca^{2+}]_i$. *B*, From a cell marked by a *circle* in the images in *A*, the fluorescence ratio 340:380 nm ($F_{340}/F_{380}$) was determined while ATP was applied. The frames in *A* were sampled at the time points indicated by the *four vertical bars*. *C*, Simultaneous currents were measured with the perforated-patch technique from the same cell, with the membrane clamped at −70 mV. A sequence of brief voltage steps in hyperpolarizing and depolarizing direction was applied every 6 sec as described for Figure 3.

versal potential of the two current responses. However, as seen in Figure 5, *C* and *D*, the conductance of the ATP response in $Ca^{2+}$-free solution was markedly reduced (mean = 67%; $n = 4$). These data imply that the first current component is due to the activation of a cation conductance, and the second to the activation of a $K^+$ conductance.

*Relative potencies of ATP, ADP, AMP, and adenosine*

To determine the type of purinergic receptor involved, we tested other purines that differentially act on different purinergic receptors. The application of 100 μM ADP activated an outwardly rectifying current component with a time course similar to the second current component activated by ATP in a subpopulation of the microglial cells (Fig. 6*B*,*C*). Out of 23 cells, 12 responded, which suggests that the present receptor has a lower affinity for ADP than for ATP and/or ADP binding to the receptor results in only part of the postreceptor events as observed for ATP binding. The characteristics of the response were variable; in seven cells a conductance increase between 1.3 and 1.6 pS was noted and the extrapolated reversal potential was around −70 mV, close to the $K^+$ equilibrium potential (Fig. 6*B*). In the remaining responsive cells the response was similar to the ATP-induced changes (Fig. 6*C*). AMP ($N = 9$) or adenosine ($N = 5$) did not result in any measurable current activation at −70 mV (Fig. 6*A*). On the same cells, ATP activated inward currents.

*Intracellular calcium responses*

Application of 100 μM ATP resulted in an increase in $[Ca^{2+}]_i$ with rise times of 10–16 sec and a slow decay over about 10 min (Fig. 7; 58 of 60 cells in three experiments). Simultaneous patch-clamp recordings showed the same characteristics as in the previous experiments during application of repetitive voltage steps from a holding potential of −70 mV. The current preceded the $Ca^{2+}$ response by few seconds. The threshold concentration for the $Ca^{2+}$ response was found at about $10^{-6}$ M ATP. A dose–response curve is given in Figure 8*A*, and in *B* an example of the responses of one cell to increasing concentrations of ATP. To test for the presence of $Ca^{2+}$ channels, cells were depolarized by increasing bath $[K^+]$ from the resting level of 5.4 mM to 55 mM. There was no apparent change in the level of intracellular $[Ca^{2+}]$. This result indicates a lack of voltage-activated $Ca^{2+}$ channels in the microglial cells (Fig. 9*B*). In the $Ca^{2+}$-free bathing solution, ATP did not elicit a change in $[Ca^{2+}]_i$; cells were superfused with the $Ca^{2+}$-free solution for 10 min prior to application of ATP. As in the patch-clamp experiments, purine analogs of ATP were used to determine whether the calcium response to ATP is mediated by the same receptor subtype. Adenosine and AMP evoked no measurable responses; however, ADP elicited a fast transient rise in $[Ca^{2+}]_i$ in 22 of 60 cells in three experiments. Neither AMP nor adenosine elicited any response in 40 cells (Fig. 9*C*).

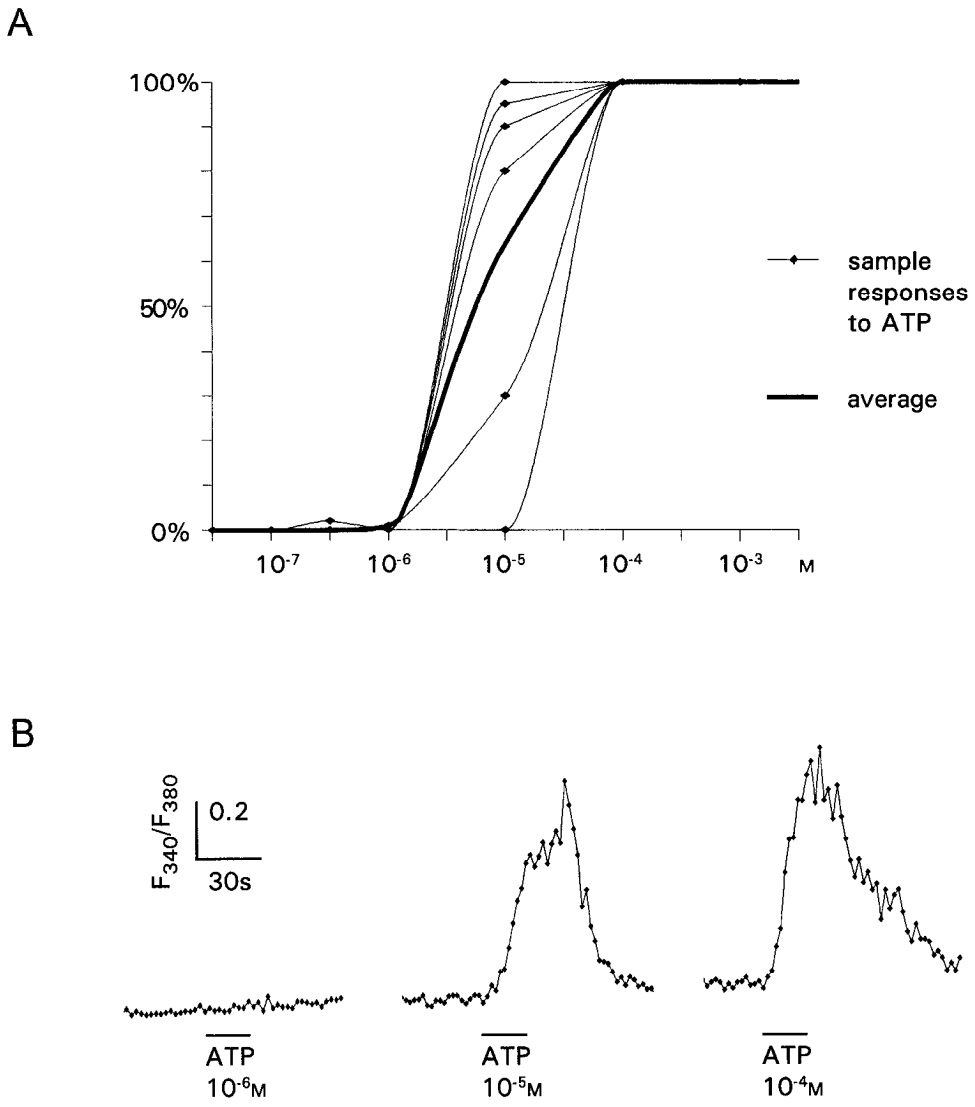


*Figure 8.* Dose–response relationship for the change in $Ca^{2+}$. *A*, Dose–response curve for the change in $[Ca^{2+}]_i$ induced by ATP ($10^{-7}$ M to $10^{-3}$ M) as determined by fura-2 fluorescence measurements. The threshold response was around $10^{-6}$ M, and the maximal response ($F_{340}/F_{380}$) was reached at $10^{-5}$ M ATP. *B*, Example of responses from one cell to increasing concentrations of ATP as indicated by changes of the $F_{340}/F_{380}$ ratios after application of ATP for 20 sec.

## Discussion

*Decrease of the ATP response with repeated applications*

Part of the ATP-evoked current is transient. This is usually a sign that the ATP response is desensitizing. Thus, the first, short-lasting (<5 min) phase of the suppression of the ATP response after repeated application in Figure 2 is in all likelihood based on a desensitization process, although an effect of the intracellular calcium increase also has to be taken into consideration. This might be an activation of an inward current with a following refractory period or an inhibition of this current by the calcium ions. These possibilities would also be consistent with the kinetics of the intracellular calcium changes as observed with the imaging system. The desensitization, therefore, is not lasting longer than 5 min. There is another possibility, however, that there might be an activation of voltage-dependent $K^+$ currents by an increased intracellular $Ca^{2+}$ concentration (Rudy, 1988). This $Ca^{2+}$ increase could be refractory to repeated stimulation within a short time frame. An increase in intracellular $Ca^{2+}$ could also inhibit $K^+$ currents as has been suggested for Bergmann glial cells (Müller et al., 1992). The longer-lasting suppression must then be considered as a rundown of the ATP response due to washout of the cytoplasm by the patch pipette solution and is a strong sign for the involvement of a second messenger in the ATP response.

*Involvement of a nonselective channel*

Studying current–voltage relationships during and after application of ATP revealed that ATP induced two different current components. The first event has a reversal potential at about 0 mV, suggesting the involvement of a nonselective conductance. Moreover, if $Na^+$ is replaced by choline or $K^+$, the reversal potential of this ATP-induced current component shifts to negative values or stays close to 0 mV, respectively, as expected for an $Na^+$- and $K^+$-permeable conductance. Removal of $Ca^{2+}$ and $Cl^-$ had no effect on the reversal potential. Despite the influx of $Ca^{2+}$ evoked by ATP, one has to conclude that the amount of $Ca^{2+}$ entering the cell is too small to contribute significantly to the membrane currents. Thus, these findings point to the activation of a cation conductance, similar to the ATP-evoked cation conductance in vascular and smooth muscle cells (Nakazawa and Matsuki, 1987), skeletal muscle (Kolb and Wakelam, 1983), and neurons (Krishtal et al., 1988). There is, however, one problem remaining: the removal of $Na^+$ leads to

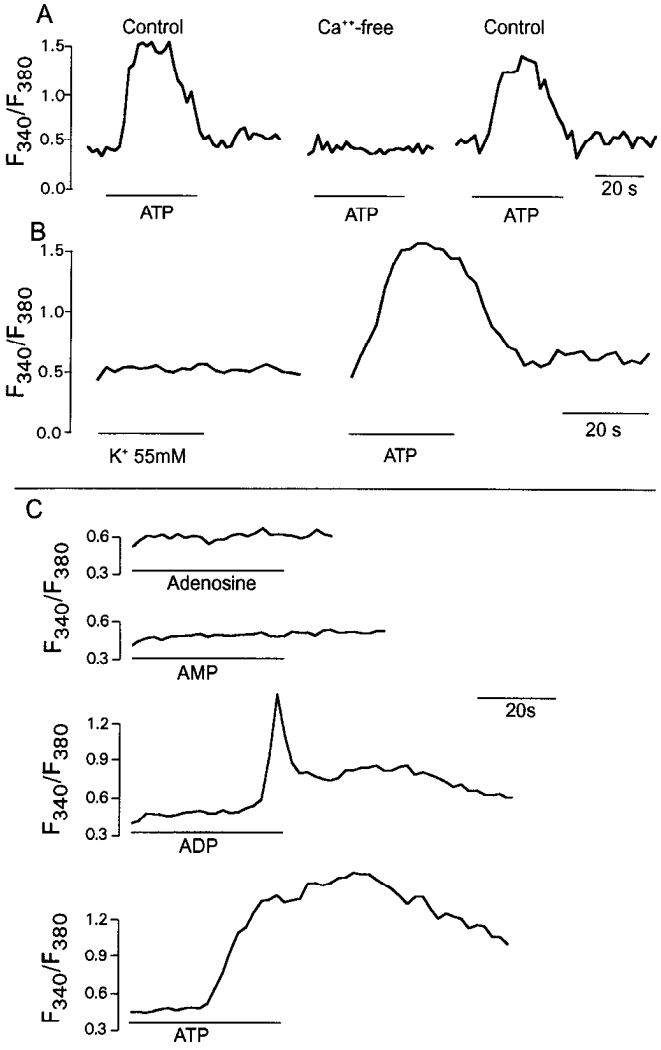


*Figure 9.* Properties of the ATP-induced $Ca^{2+}$ changes. *A*, The ATP-induced changes in the fluorescence ratio $F_{340}/F_{380}$ reflecting changes in internal $Ca^{2+}$ were compared in normal bathing solution (*left* and *right traces*) with responses in $Ca^{2+}$-free solution (*middle trace*). The ATP response is abolished in $Ca^{2+}$-free solution. *B*, To determine whether voltage-dependent $Ca^{2+}$ channels are involved, a depolarizing bath solution containing 55 mM $K^+$ was used to superfuse the cells for 20 sec. Depolarization did not induce a change in $[Ca^{2+}]_i$. The cells responded with $Ca^{2+}$ influx to control application of ATP (*left trace*). *C*, A typical example of responses of one cell to adenosine nucleotide analogs. Compounds were applied at $10^{-4}$ M (except for ATP, $10^{-5}$ M) for 40 sec and fura-2 ratio values were obtained every 2 sec. $[Ca^{2+}]_i$ did not change in response to adenosine or AMP. ADP induced a biphasic response with a fast transient component followed by a more sustained $[Ca^{2+}]_i$ elevation. Addition of ATP resulted in a slower increase in $[Ca^{2+}]_i$ sustained over several minutes before it returned to resting values.

a drastic conductance decrease, which can only be explained if one assumes that the channel permeability is controlled by the availability of $Na^+$. An increase of the $K^+$ concentration can only partially substitute for the $Na^+$-dependent conductance.

*Involvement of a $K^+$ channel*

The second current component has a delayed onset and lasts for many seconds. The current–voltage relation indicates an outwardly rectifying current component with an extrapolated reversal close to the $K^+$ equilibrium potential, indicating the activation of an outwardly rectifying $K^+$ channel. As expected for a $K^+$-selective conductance, the reversal potential is affected by a change in the $K^+$ equilibrium potential. Voltage- and calcium-activated channels have been described in the literature (Rudy, 1988). In microglial cells this $K^+$ channel must be constitutively present, although suppressed under the present culture conditions. Activation of ATP receptors by ATP or ADP leads to a transient activation of this current.

*Nature of the receptor*

Since AMP and adenosine do not have any effect on the cation channel, one has to conclude from these relative studies that the mechanism works via a $P_2$ purinoreceptor. A biphasic $P_2$ purinoreceptor response was found in at least two other preparations. In smooth muscle a fast calcium inward current is followed by a transient $K^+$ outward current (Mollemann et al., 1989), and in skeletal muscle a large cation conductance increase is followed by a transient $K^+$ outward current (Hume and Thomas, 1988). None of these receptors were characterized further to determine the receptor subtype(s). The response to ADP was variable. The affinity of ADP to the receptor appeared to be lower than for ATP, which is consistent with the expression of a $P_2$ receptor. There might also be a second receptor involved, whose expression does not completely overlap with the ATP receptor that mediated the responses described in this publication. A possibility would be that there are receptors expressed that are only sensitive to ADP similar to the $P_{2T}$ receptors expressed on platelets (Gordon, 1986).

*Functional implications*

The ATP-evoked inward current has the potential to act as an activation signal for microglial cells. Due to the lack of outward $K^+$ currents under resting conditions, the opening of the ATP-dependent cationic conductance will lead to a substantial and long-lasting depolarization. The delayed onset of the outwardly rectifying $K^+$ current could serve to restore the membrane potential similarly as for the action potential, but on a several thousand-fold longer time scale.

The ATP-mediated depolarization should lead to an inhibition of $Na^+$-dependent carriers, like $Na^+/H^+$ exchange, and therefore could evoke an acidification. This, together with the observed increase in $Ca^{2+}$, could act as a signal for transition from one functional state of microglial cells into another. Larger amounts of extracellular ATP signal pathological events like ischemia and injury, and this transmitter may be the molecular link between injured neurons and microglial cells.

## References

Banati R, Hoppe D, Gottmann K, Kreutzberg GW, Kettenmann H (1991) A sub-population of bone marrow derived macrophages share a unique ion channel pattern with microglia. J Neurosci Res 30:593–600.

Burnstock G (1990) Overview: purinergic mechanisms. Ann NJ Acad Sci 603:1–17.

Cameron DJ (1984) Inhibition of macrophage mediated cytotoxicity by exogenous adenosine 5′ triphosphate. J Clin Lab Immunol 15: 215–218.

di Virgilio F, Pizzo P, Picello E (1991) Mechanisms of neutrophil and macrophage motility. Adv Exp Med Biol 297:13–22.

Forrester T, Williams CA (1977) Release of adenosine triphosphate from isolated adult heart cells in response to hypoxia. J Physiol (Lond) 268:371–390.

Frei K, Siepl C, Groscurth P, Bodmer S, Schwerdel C, Fontana A (1978)

Antigen presentation and tumor cytoxicity by interferon-gamma-treated microglial cells. Eur J Immunol 17:1271–1278.
Gallin EK, Gallin JI (1977) Interaction of chemotactic factors with human macrophages: induction of transmembrane potential changes. J Cell Biol 75:277–289.
Gallin EK, Sheehy PA (1985) Differential expression of inward and outward potassium currents in the macrophage-like cell line J7774. J Physiol (Lond) 369:475–499.
Gehrmann J, Gold R, Linington C, Lannes-Vieira J, Wekerle H, Kreutzberg GW (1992) Spinal cord microglia in experimental allergic neuritis: evidence for fast and remote activation. Lab Invest 67:100–113.
Giulian D, Baker TJ (1986) Characterization of ameboid microglia isolated from developing mammalian brain. J Neurosci 6:2163–2178.
Giulian D, Ingeman JE (1988) Colony-stimulating factors as promotors of ameboid microglia. J Neurosci 8:4707–4717.
Gordon JL (1986) Extracellular ATP: effects, sources and fate. Biochemistry 233:309–319.
Graeber MB, Banati RB, Streit WJ, Kreutzberg GW (1989) Immunophenotypic characterization of rat brain macrophages in culture. Neurosci Lett 103:241–246.
Hamill OP, Marty A, Neher E, Sakmann B, Sigworth FJ (1981) Improved patch-clamp techniques for high-resolution current recording from cells and cell-free membrane patches. Pfluegers Arch 391:85–100.
Hume RI, Thomas SA (1988) Multiple actions of adenosine 5'-triphosphate on chick skeletal muscle. J Physiol (Lond) 406:503–524.
Imai S, Riley AL, Berne RM (1964) Effect of ischemia on adenine nucleotides in cardiac and skeletal muscle. Circ Res 15:443–450.
Kettenmann H, Hoppe D, Gottmann K, Banati R, Kreutzberg GW (1990) Cultured microglial cells have a distinct pattern of membrane channels different from peritoneal macrophages. J Neurosci Res 26: 278–287.
Kolb HA, Wakelam MJO (1983) Transmitter-like action of ATP on patched membranes of cultured myoblasts and myotubes. Nature 303: 621–623.
Korn SJ, Marty A, Connor JA, Horn R (1991) Perforated patch recording. Methods Neurosci 4:364–373.
Kreutzberg GW (1978) 5'Nucleotidase of microglial cells in the facial nucleus during axonal reaction. J Neurocytol 7:601–610.
Krishtal OA, Marchenko SM, Obukhov AG (1988) Cationic channels activated by extracellular ATP in rat sensory neurons. Neurosci 27: 995–1000.
Kruskal BA, Maxfield FR (1987) Cytosolic free calcium increases before and oscillates during frustrated phagocytosis in macrophages. J Cell Biol 105:2685–2693.
Kruskal BA, Shak S, Maxfield FR (1986) Spreading of human neutrophils is immediately preceded by a large increase in cytoplasmic free calcium. Proc Natl Acad Sci USA 83:2919–2923.
Leist TP, Frei K, Kam-Hansen S, Zinkernagel RM, Fontana A (1988) Tumor necrosis factor-alpha in cerebrospinal fluid during bacterial, but not viral, meningitis. Evaluation in murine model infections and in patients. J Exp Med 167:1743–1748.
Meagher LC, Moonga BS, Haslett C, Huang CL, Zaidi M (1991) Single pulses of cytoplasmic calcium associated with phagocytosis of individual particles by macrophages. Biochem Biophys Res Commun 177:460–465.
Metcalfe JC, Moore JP, Smith GA, Hesketh TR (1990) Calcium and cell proliferation. Br Med Bull 42:405–412.
Mollemann A, Nelemans A, Den Hertog A (1989) $P_2$-purinoreceptor-mediated membrane currents in DDT, MF-2 smooth muscle cells. Eur J Pharmacol 169:167–174.
Müller T, Möller T, Berger T, Schnitzer J, Kettenmann H (1992) Calcium entry through kainate receptors and resulting potassium-channel blockade in Bergmann glial cells. Science 256:1563–1566.
Nakazawa K, Matsuki N (1987) Adenosine triphosphate-activated inward current in isolated smooth muscle cells from rat vas deferens. Pfluegers Arch 409:644–646.
Perry VH, Gordon S (1988) Macrophages and microglia in the nervous system. Trends Neurosci 11:273–277.
Ramon y Cajal S (1914) Estudios sobre la degeneracion y regeneracion systema nervioso, Vol 2, Degeneracion y regeneracion de los centros nerviosos. Madrid: Moya.
Rephaeli A, Aviram A, Rabizadeh E, Shaklai M (1990) Proliferation-associated changes of $Ca^{2+}$ transport in myeloid leukemic cell lines. J Cell Physiol 143:154–159.
Rudy B (1988) Diversity and ubiquity of K channels. Neurosci 25: 729–749.
Steinberg TH, Silverstein SC (1987) Extracellular $ATP^{4-}$ promotes cation fluxes in the J774 mouse macrophage cell line. J Biol Chem 262:3118–3122.
Streit WJ, Graeber MB, Kreutzberg GW (1988) Functional plasticity of microglia: a review. Glia 1:301–307.
Streit WJ, Graeber MB, Kreutzberg GW (1989) Expression of Ia antigen on perivascular and microglial cells after sublethal and lethal motor neuron injury. Exp Neurol 105:115–126.
Trotter J, Bitter-Suermann D, Schachner M (1989) Differentiation-regulated loss of the polysialylated embryonic form and expression of the different polypeptides of the neural cell adhesion molecule (N-CAM) by cultured oligodendrocytes and myelin. J Neurosci Res 22: 369–383.